DAEHAN HWAHAK HWOEJEE
(*Journal of the Korean Chemical Society*)
Vol. 30, No. 3, 1986
Printed in the Republic of Korea

유도결합 플라스마 공간내의 전자밀도 분포

崔 範 錫
경희대학교 자연과학대학 화학과

(1986. 2. 24 접수)

Spatial Distribution of Electron Number Density in an Inductively Coupled Plasma

Beom Suk Choi
Department of Chemistry, Kyunghee University Yongin 170-73, Korea

(Received February 24, 1986)

요 약. 유도결합 플라스마 공간내의 전자밀도를 측정하였다. 전자밀도의 측정시 유도결합 플라스마의 작동조건은, (1) 냉각기체만 사용할 때, (2) 냉각기체와 운반기체만을 사용할 때, (3) 보통의 작동조건, 즉 에아로졸을 포함한 운반기체를 사용할 때, (4) 약 88%의 에아로졸을 제거시켰을 때, 그리고 (5) 과량의 리튬을 주입시켰을 때로서 분류하였다. 보통의 작동조건에서 플라스마의 낮은 부분에서는 전자밀도가 상당히 감소하여 플라스마내의 가장 전자밀도가 큰 곳보다 약 80배 감소하였다. 이온화 방해영향을 일으키는 알칼리금속을 과량으로 넣었을 때 전자밀도의 변화는 관찰되지 않았고 유도코일의 power를 증가시키면 전자밀도도 증가하였다.

ABSTRACT. Spatial (radial and height) distribution of electron number density is measured for an inductively coupled plasma under five operating conditions: (1) no carrier gas, (2) carrier gas without aerosel, (3) carrier gas with aerosol, (4) carrier gas with desolvated aerosol, and (5) carrier gas with aerosol and excess lithium. A complete RF power mapping of electron density is obtained. The plasma electrons for a typical analytical torch are observed to be hollow at the radial center in the region close to the induction coil, but diffuse rapidly toward the center in the higher region of the plasma. The presence of excess Li makes no significant change in the electron density profiles. The increases in the RF power levels increase the values of electron density uniformly across the radial coordinate.

INTRODUCTION

The inductively coupled plasma (ICP) has become widely used as an excitation source for an atomic emission spectrometry. The advantages often cited are its apparent high temperature and inert argon atomosphere. However, recent works have demonstrated that the interelement effect not only exists in the ICP, but also analytical optimization process is a complex function of operating parameters[1~2]. To optimize the operating conditions of the ICP, the excitation mechanisms of the analyte were studied by many workers[3~10], and the brief description of the existing mechanisms recently reviewed by Galan[3]. However, in order to support the proposed analyte excitation mechanisms, quantitative data on the spatial distributions of plasma electron and argon excitated states including metastable states should be fully characterized.

In the present work, using a commercial plasma torch commonly employed for analytical application, the radial electron density profiles at three plasma heights and three power levels under five operating conditions were determined. The five operating conditions were selected in order for the analyst to be able to deduce the electron number density when the operating condition varied, and they are (1) no carrier gas, (2) carrier gas without aerosol, (3) carrier gas with aerosol (normal operating condition) (4) carrier gas with desolvated aerosol, and (5) carrier gas with aerosol and excess lithium.

The electron densities were calculate from the observed Stark broadening of the hydrogen beta line (H_β, 486.1 nm). Electron number densities are presented in radial and height coordinates with errors properly analyzed. The operating parameters of the plasma are the same as that in the previous analyte studies.[11]

EXPERIMENTAL AND PROCEDURE

Instrumental: The plasma system used was the Plasma Therm ICP-2500 (Plasma Therm Inc., Kresson, N.J.). The cross flow nebulizer, spray chamber and torch used were supplied by the same manufacturer. The RF generator is of crystal-controlled type operating at the frequency of 27.12MHz. The torch used in this study consists of three concentric quartz tubes with a 18mm *i.d.* (inside diameter) in the outer tube, a 12mm *i.d.* in the intermediate tube and 1.5 mm *i.d.* in the central aerosol channel.

The spectrometer was built around a Hilger Engis model 1000 Czerny-Turner grating monochromater and has been described previously by Koirtyohann and his coworkers[12]. In this configuration, the plasma torch lies horizontal with respect to the vertical entrance slit of the monochromater and the vertical movement of a mask with a small opening allows the lateral scanning of the plasma at a given plasma height. The height of plasma being observed is changed by sliding the torch horizontally. A two fold image reduction lens was placed before the entrance slit; so that the mask opening of 0.1mm and the vertical drive in steps of 0.1 mm provide spatial resolution of 0.2mm at the center of plasma. With the above arrangement the detector response was observed to be fairly constant for lateral distances of ±6mm. Lateral emission intensities were measured within ±8 mm from the plasma center. The estimated resolution of the spectrometer at 450mm is about 0.016nm with the entrace slit held at 20μm.

For the measurement of electron number density without the carrier gas, the hydrogen source for the H_β line emission was introduced when a portion of coolant gas was bubbled through water and added into the main coolant gas channel. Introducing water into the coolant gas reduces the electron density in the plasma. The amount of water added was gradually reduced until no further reduction of electron density was observed. The optimal condition was obtained by adding argon gas saturated with water at room temperature to the coolant gas at the rate of 0.04*l*/min while the coolant gas flow itself was maintained at 15*l*/min. The same arrangement served as the hydrogen source for the plasma configuration without analyte aerosol. For the normal operation of the plasma, the amount of analyte solution delivered to the torch was about 0.030m*l*/min. A separate hydrogen source for the H_β line emission was not needed, since the aerosol provided more than enough water into the torch. For the desolvation studies[11], the carrier gas aerosol was passed through the heater and condensor combination to trap the excess water. Up to 88% of water was trapped by this arrangement. The concentration of excess Li added to our analyte solution was 1000

$\mu g/ml$. The operating conditions chosen for this study were $15l$/min coolant flow, $1.1l$/min aerosol flow and zero auxillary flow. The RF power was maintained at 1.25kw unless otherwise specified. At this operation conditions, the tip of the initial radiation zone[12] was observed at 13mm above the induction coil.

Electron number density measurement: The halfwidth measurement of a Starkbroadened line is one of the most accurate and convenient methods of determining the electron number density, n_e in a dense plasma, and the basis of this measurement can be found in standard texts[13,14]. Kalnicky *et al.*[15] reviewed its application to the anlytical plasma in conjunction with the method of Saha-Eggert ionization equilibria. The Stark-broadened linewidth is related to the value of n_e in the plasma by[16] ; $n_e=C(T, n_e)(\lambda_{1/2})^{3/2}$. The constant $C(T, n_e)$ is a slowly varying function of both parameters and is extensively tabulated[14,17]. For the hydrogen beta line, its halfwidth varies little with the temperature between 5×10^3 and 4×10^4K and a graph is drawn so that the n_e values can be read directly from the experimental value of $\lambda_{1/2}$[13].

The source of hydrogen in the plasma is the decompostion of water added to the coolant gas or the aqueous solution nebulized with the carrier gas. For the first two operating configurations, no carrier gas and carrier gas without aerosol (carrier gas bypasses the nubulizer), a minimal amount of water is added to the coolant gas. The radial emission profiles of the H_β line at three plasma heights, 4, 10 and 16mm above the induction coil are shown in *Fig.* 1a. For the next three configurations, aerosol from the nebulizer is the source of the hydrogen for the H_β emission. Their radial peak emission profiles are shown in *Fig.* 1b.

The lateral H_β emission intensity, $I(\lambda, x)$ was measured at wavelength intervals of 0.1nm in the plasma region where the observed halfwidth is in the order of 0.5nm. Intervals as small as 0.02nm were used when the observed halfwidth narrowed down to 0.05nm. Each lateral profile, $I(\lambda, x)$ was inverted to form a radial profile $I(\lambda, r)$ by using the Abel inversion method described previously[18] (*Fig.* 2). The Abel inversion program fits the observed lateral intensity data to a symmetrical function,

$$I(\lambda, x)=[c_2+c_3(x-c_1)^2+c_4\ (x-c_1)^4].$$

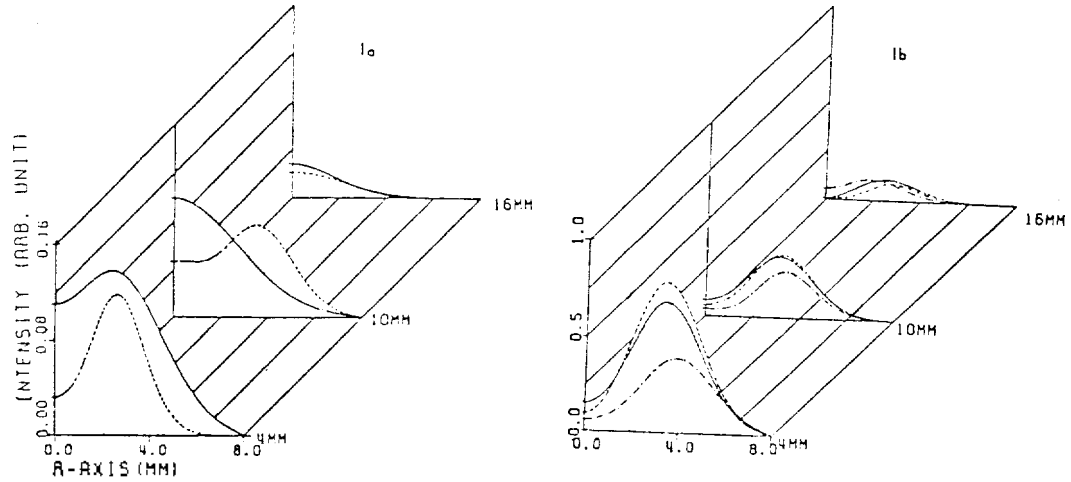

Fig. 1. Radial emission profiles of the H_β line (486.13nm) at 4, 10, and 16mm above the induction coil. RF power at 1.25kw. (a) no carrier gas (—) and carrier gas without aerosol (···). (b) Normal operation of plasma (—), with excess Lithium (···) and desolvated (-·-·-·-·-).

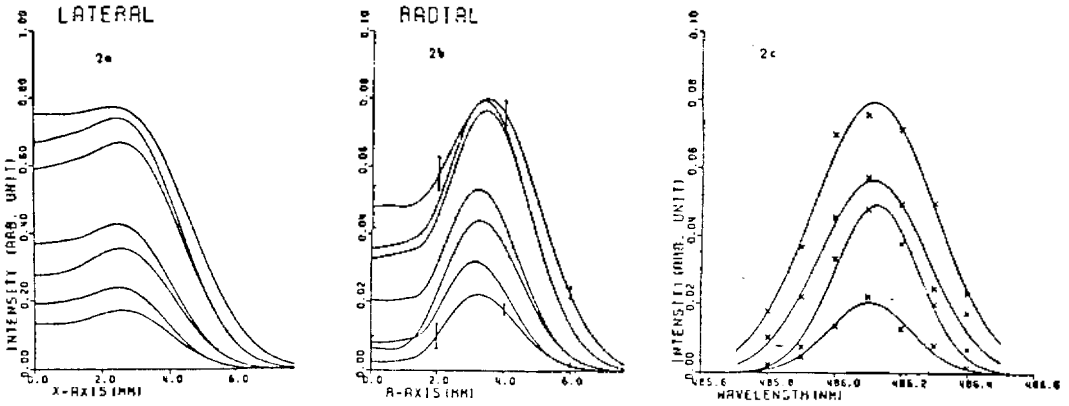

Fig. 2. Stark-broadened H_β line profiles at the 10mm above the induction coil: carrier gas without aerosol. The intensities are measured between 485.8 and 486.4 nm at every 0.1nm intervals. RF power at 1.25kw. (a) lateral intensity profiles. The most intense profile belongs to 486.1nm. (b) radial intensity profiles. The order of intensities are same as that of the lateral profiles. (c) radial intensities vs. wavelengths at the radial distance intervals of 2mm; radial distance of 4.0, 2.0, 0.0 and 6.0mm are shown from the top.

$$\exp(-c_5(x-c_1)^2)$$

by the least squares, and the function is then numerically inverted into a radial profile. This method allows proper analysis of error propagation. A set of lateral profiles, $I(\lambda, x)$ of the H_β line measured at wavelength intervals of 0.1 nm for an analytical plasma are shown in *Fig.* 2a and the corresponding radial profiles, $I(\lambda, r)$ are shown in *Fig.* 2b. The lateral background emission intensity measured at 485.0nm was substracted from all of the lateral emission profiles before Abel inversion. For a given radial coordinate r, the $I(\lambda, r)$ values as shown in *Fig.* 2c were fitted to a Gaussian lineshape function by the method of least squares. The instrumental resolution and the Doppler width contribute to the halfwidth; they were estimated to be 0.016nm[12] and 0.027nm[16](for plasma temperature of 6000K). The combined halfwidth, $\Delta\lambda_{1/2}$, was substracted from the halfwidth of H_β line using the relation $(\Delta\lambda_{1/2})^2=(\Delta\lambda^d_{1/2})^2+(\Delta\lambda^i_{1/2})^2$, where $\Delta\lambda^d_{1/2}$ and $\Delta\lambda^i_{1/2}$ are the Dopper and instrumental halfwidth respectively.

Two major sources of error are associated with the data reduction. The first is the uncertainty arising from the Gaussian fits to the halfwidth. It ranges from 7 % to 17 % depending on the halfwidth, smaller halfwidth having the larger percent error. The second is the error associated with the Abel inversion. It is the smallest(about 8 %) near the radial intensity maxima, and largest (as high as 30 %) near the center of the hollow plasma. For the plasma profiles where the radial intensity does not dip at the center, a uniform error of 8 % is found. Experimental uncertainties are indicated in figure 2b. In addition, about 10 % uncertainty for the theoretical treatments of the H_β Stark-broadening method should be considered[14]. Therefore, the cumulative errors are of the order of 25 % for the flatest regions of the electron density profiles and then increase to about 60 % near the radial center where the electron density drops sharply.

RESULT AND DISCUSSION

The electron number density profiles under five operating conditions and three power variations are shown in *Fig.* 3. The electron number density profiles shown in *Fig.* 3a~3c show

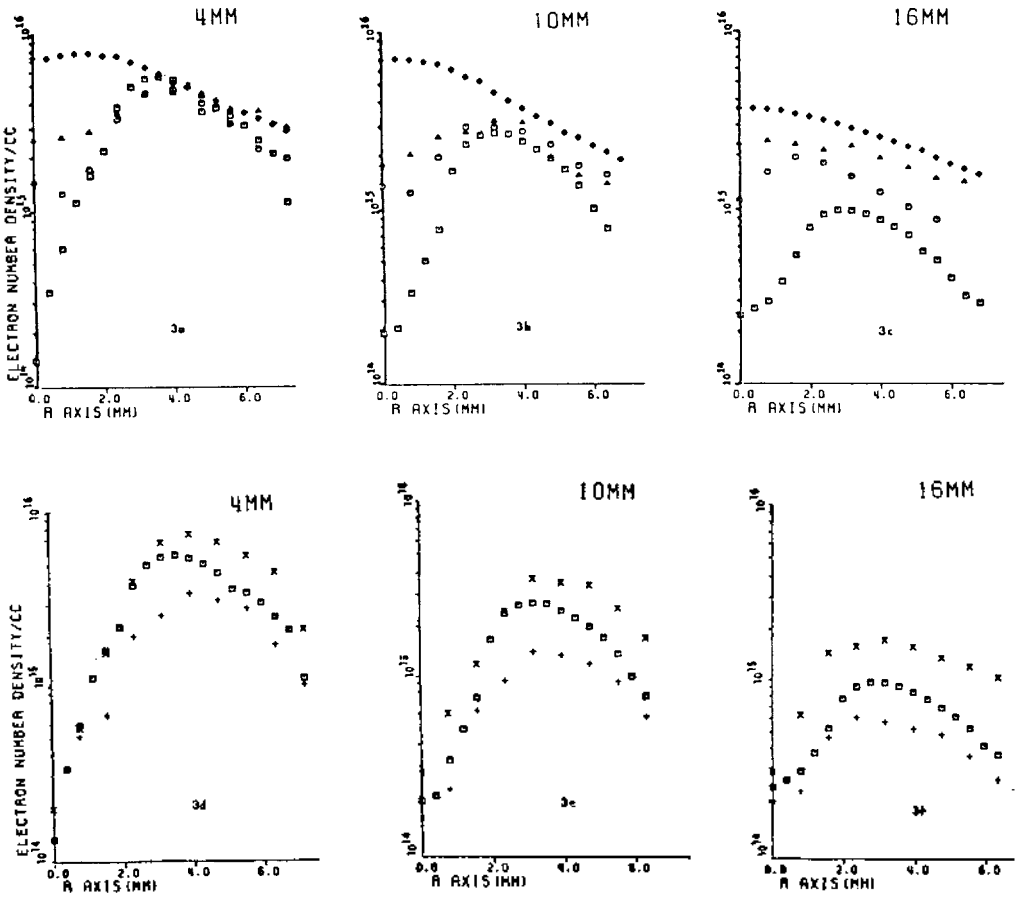

Fig. 3. Electron number density profiles at three plasma heights, 4, 10 and 16mm above the induction coil. 3a thru 3c represent constant RF power (1.25kw) profiles of no carrier gas (◇), carrier gas without aerosol (△), desolvated (○) and normal operating condition (□). 3d thru 3e are profiles of normal operating condition at three RF power levels; 1.5 (X), 1.25 (□) and 1.0 (+) kw.

that the electron numbers at 4m above the induction coil and 4~5mm from the radial center are relatively same regardless of operating conditions. It suggests the plasma is not disturbed by the carrier gas argon stream or the aerosol at the induction zone[12].

The electron density profile is fairly uniform ($4\times10^{15}\sim8\times10^{15}$) across the radial center when the carrier gas is turned off, but it has a small depression at the radial center when the carrier gas is turned on. The centeral depression is steepest at the preheating zone[12] (4mm above induction coil at radial center) where cold aerosol gas are introduced to the torch, and it recovers slowly in relation to the radial maximum at upper plasma height.

The electron number density profile under nomal operating condition shows sharp depression at the radial center regardless of plasma height. Its number densities are depressed as low as $1\times10^{14}\sim3\times10^{14}$. For desolvated studies, electron number density ranged between that of with and without aerosol.

The electron number density profile when excess lithium present is not included in *Fig.* 3a~3c. Although the excess lithium in the aero-

sol presented small changes in hydrogen beta line intensities, a small enhancement at the plasma height of 4mm and a small supression at the plasma height of 16mm as shown in *Fig.* 1b, it made no observable change in the electron density profile. The similar observation had been reported by Kalnicky *et al.* who observed the electron number density at the higher region of the plasma when excess sodium was present or not[15]. These observations are unexpected since the analyte intensity is influenced by the easily ionizable element such as lithium and sodium[10], and it does not support the predominantly proposed mechanism of ambipolar diffusion model. However, considering the uncertainty range of electron number densities with excess lithium are well within the uncertainty range under the normal operating condition, proposed ambipolar difusion model should not be rejected.

The dependence of the electron density upon RF power level is shown in *Fig.* 3d~3f for the plasma operating condition of carrier gas without aerosol. Fairly uniform increase in the electron density is observed at all three plasma height with corresponding increase in RF power level. The observation partly supports the model of the collisional excitation by electron since the analyte intensity is increased by the increase of the electron number density[9].

REFERENCES

1. P. W. J. M. Boumans and F. J. DeBoer, *Spectrochim. Acta* **31B**, 355 (1976).
2. G. R. Kornblum and L. Degalan, *Spectrochim, Acta,* **32B**, 455 (1977).
3. L. Degalan, *Spectrochim. Acta,* **39B**, 537 (1984).
4. P. W. J. M. Boumans and F. J. DeBoer, *Spectrochim. Acta,* **32B**, 365 (1977).
5. M. W. Blades and G. M. Hieftje, *Spectrochim. Acta,* **37B**, 191 (1982).
6. M. W. Blades, *Spectrochim. Acta,* **37B**, 869 (1982).
7. R. J. Lovett, *Spectrochim. Acta,* **37B**, 969 (1982).
8. F. Aeschbach, *Spectrochim. Acta,* **37B**, 987 (1982).
9. M. W. Blades and G. Horlick, *Spectrochim. Acta,* **36B**, 861 (1981).
10. M. W. Blades and G. Horlick, *Spectrochim. Acta,* **36B**, 881 (1981).
11. J. Rybarczyk, ph. D. thesis, University of Missouri, columbia, MO. U. S. A. (1981).
12. S. R. Koirtyohann, J. S. Jones, C. P. Jester and D. A. Yates, *Spectrochim. Acta,* **36B**, 49 (1981).
13. R. H. Huddlestone and S. L. Leonard, Plasma Diagnostic Techniques, Academic Press, New York, N. Y (1965).
14. H. R. Griem, Spectral Line Broading By Plasmas, Academic Press, New York, N. Y (1974).
15. D. J. Kalnicky, V. A. Fassel and R. N. Kniseley, *Appl. Spectrosc.* **31**, 139 (1980).
16. J. F. Alder, R. M. Bombelka and G. F. Kirkbright, *Spectrochim. Acta,* **35B**, 163 (1980).
17. C. R. Vidal, J. Cooper and E. W. Smith, *Astrophys. J. Supp. Ser.* **25**, 37 (1973).
18. B. S. Choi and H. Kim, *Appl. Spectrosc.* **36**, 71 (1982).